Available online at BCREC website: https://bcrec.id

Bulletin of Chemical Reaction Engineering & Catalysis, 16 (3) 2021, 651-660

Research Article

A New Approach for the Green Biosynthesis of Silver Oxide Nanoparticles Ag_2O, Characterization and Catalytic Application

Brahim El-Ghmari*, Hanane Farah, Abdellah Ech-Chahad

Physical-Chemistry of Processes and Materials Laboratory, Faculty of Science and Technology, Hassan First University of Settat, 26000 Settat, Morocco.

Received: 28th June 2021; Revised: 14th July 2021; Accepted: 15th July 2021
Available online: 17th July 2021; Published regularly: September 2021

Abstract

In this paper, a facile and green approach for the synthesis of silver oxide nanoparticles Ag_2O NPs was performed using the extract of the wild plant *Herniaria hirsuta* (*H. hirsuta*). Different spectral methods were used for the characterization of the biosynthesized Ag_2O NPs, ultraviolet-visible (UV-Vis) spectroscopy gave a surface plasmon resonance (SPR) peak of Ag_2O NPs is 430 nm, estimation of direct and indirect forbidden gap bands are respectively 3.76 eV and 3.68 eV; Fourier transform infrared (FTIR) spectral analysis revealed the groups responsible for the stability and synthesis of Ag_2O NPs. The morphology of Ag_2O NPs was studied by scanning electron microscopy (SEM) showing a nearly spherical shape of Ag_2O NPs, and X-ray diffraction (XRD) study confirmed the crystallinity of Ag_2O NPs with a crystallinity size of 15.51 nm. The catalytic activity of Ag_2O NPs, as well as the rings number were studied by the degradation of methylene blue dye.

Keywords: Silver oxide Ag_2O nanoparticles; *Herniaria hirsuta*; Silver nitrate $AgNO_3$; Dye degradation

How to Cite: B. El-Ghmari, H. Farah, A. Ech-Chahad (2021). A New Approach for the Green Biosynthesis of Silver Oxide Nanoparticles Ag_2O, Characterization and Catalytic Application. *Bulletin of Chemical Reaction Engineering & Catalysis*, 16(3), 651-660 (doi: 10.9767/bcrec.16.3.11577.651-660)

Permalink/DOI: https://doi.org/10.9767/bcrec.16.3.11577.651-660

1. Introduction

Nanotechnology is defined as "the creation and use of structures, devices, and systems characterized by their distinct and varied characteristics and infinitesimal size, typically to deal with particles in the size range 1-100 nm [1]. At these scales, the material acquires properties that are unusual and often different from those of the same materials in bulk: they should be considered as new chemical compounds with different toxicities and characteristics [2]. Recently, silver-based nanomaterials have been widely considered as antimicrobial agents [3–7]. Silver oxide nanoparticles can have different applications in the form of sensors [8], photovoltaic cells [9], catalysts [10], and fuel cells [11]. These products can also be practiced as important components in optical memories [9], and plasmonic photonic devices [12]. Researchers and specialists have predicted the great role that nanotechnology will play in the development of the developing world, so the abundance of new and revolutionary ways and means, which have contributed to advances in several fields such as energy storage and transportation, pharmaceuticals and medicine [13]. Green synthesis is a modern field of biotechnology that is environmentally friendly and economical as an alterna-

* Corresponding Author.
Email: braxgh@gmail.com (B. El-ghmari);
Telp: +212-662331049

tive to chemical and physical methods that in many cases are dangerous for the environment. Because in this method, natural reagents are biologically safe, non-toxic and environmentally friendly [14], *Ziziphora clinopodioides* [15], *Petiveria alliacea* L. [16], *Paeonia emodi* [17], Centella asiatica and *Tridax* [18], *Callistemon lanceotus* (*Myrtaceae*) [19] and many others have been used in the biosynthesis of metal oxide nanoparticles [20].

In the green synthesis of metal oxide nanoparticles, researchers have used plant extracts widely available in nature. Due to its speed, environmental efficiency and low cost, which are known as "vital plants". It has the power to absorb minerals while respecting the safety levels [21]. These methods include algae, microbes such as fungi, bacteria, and viruses as reducing agents [6,22]. The current method has more than one advantage as it is an economical technique that is solvent and surfactant-free [21].

In recent years, several studies have been conducted in the field of nanotechnology that exploits green plant materials and extracts for the biosynthesis of metal oxide nanoparticles to avoid chemicals responsible for environmental pollution. The biosynthesis of metal nanoparticles is carried out by a green method, using different plant fractions as reducing and stabilizing agents. Among the many metallic nanoparticles that have been studied, silver oxide is a valuable material used in various fields because of its unique characteristics. Therefore, it occupies great importance in the field of nanomaterials. Its characteristics are photoelectric, catalysis and drug delivery [23,24], cathode in rechargeable batteries [11]. The increase of the industrial activities implies always a great pollution of the environment by chemicals is due to an insufficiency of treatment systems, simple and less expensive solutions are then strongly required, among them we find the nanoparticles which already showed their potential in the treatment of organic pollutants such as the blue of methylene which is very used in several sectors: chemistry, pharmacology, medicine, biology, textile [25]. The ignorant use of this substance causes serious damage to human health and the environment [26,27].

In this study, for the first time silver oxide nanoparticles Ag_2O NPs were synthesized and studied by the aqueous extract of *H. hirsuta* plant. The characterizations of the obtained Ag_2O NPs nanoparticles were analyzed using standard techniques such as UV-Vis, FT-IR, XRD and SEM. In addition to a study of their optical properties and their catalytic activity for dye degradation were evaluated.

2. Materials and Methods

2.1 Materials

The precursor chemicals used were: silver nitrate $AgNO_3$ (99.9%, oxford LAB FINE CHEM. India), the plant *H. hirsuta* was harvested from the province of Ouezzane in the North of Morocco, sodium hydroxide (98%, LOBA CHEMIE PVT.LTD. India). The glassware used was washed with acetic acid and rinsed with distilled water. Two mortars one in porcelain and the other in zirconium.

2.2 Preparation of the Extract of the Plant *H. hirsuta*

The *H. hirsuta* plant was harvested during the June, dried and stored in the dark at room temperature, after about two months the *H. hirsuta* plant was washed twice with distilled water and dried at room temperature for 48 h, ground to a fine powder. 10 g of the *H. hirsuta* plant was added to 400 mL in a 500 mL beaker. The mixture was shaken vigorously at 5000 rpm and under room temperature overnight. The extract obtained was filtered through a piece of tissue and stored in a container. Finally, the filtrate was centrifuged at a speed of 10,000 rpm under room temperature to obtain a clear brown supernatant and stored in a container away from light for further use.

2.3 Biosynthesis of Silver Oxide Nanoparticles (Ag_2O NPs)

In a 250 mL beaker, 20 mL of the silver nitrate solution $AgNO_3$ (4.5 g, 0.04 mol) was added to 60 mL of the plant extract *H. hirsuta* while stirring at 5000 rpm at room temperature for 10 min. The formation of biosynthesized Ag_2O NPs was observed by the change of color and the appearance of a brown-black precipitate after a duration of 5 min and confirmed by UV-vis spectroscopy after adjusting the pH = 8 by sodium hydroxide solution (0.1 M). Finally, the mixture was centrifuged at a speed of 10,000 rpm under room temperature to remove the supernatant, the precipitate was washed twice with distilled water and methanol then dried in the oven at a temperature of 70 °C overnight, and stored in a glass container for further analysis.

2.4 Characterization of Silver Oxide Nanoparticles (Ag_2O NPs) Biosynthesized

2.4.1 UV- vis spectroscopy

The production of Ag_2O NPs was monitored using UV-visible spectroscopy

(spectrophotometer DR 6.000 with RFID technology (HACH LANGE, GERMANY). Measurements were recorded in the wavelength range of 250 to 900 nm and at room temperature. Its stability was monitored by UV-vis spectroscopy using distilled water as a control in a quartz cell.

2.4.2 X-ray Diffraction (XRD)

Crystal structure of the biosynthesized Ag_2O NPs was carried out by an X-ray powder diffractometer (Phaser D2 Diffractometer, Broker, USA), with Cu-Kα radiation of wavelength λ = 0.15406 nm in the range of 10°−80°, operating at 30 KV and 10 mA.

2.4.3 Fourier transform infrared spectroscopy FT-IR

Different functional groups were observed by FTIR spectral analysis Varian 800/Gladiatr model (Scimitar Series, Australia/Pike Technologies, USA) such as carbonyls, amines, phenols and amides which could be bioreducers for the synthesis of Ag_2O NPs.

2.4.4 Scanning electron microscopy SEM

The morphology and shape of synthesized Ag_2O NPs were studied using scanning electron microscopy coupled with EDS (SEM-JEOL IT500HR) with the following characteristics: Landing Voltage 15.0 kV, WD 11.0 mm, Magnification x800, Vacuum Mode High Vacuum.

2.5 Catalytic Activity of Biosynthesized Ag_2O NPs

2.5.1 Catalytic degradation of methylene blue dye

The silver nanoparticles obtained by the green method, tested for the reduction of methylene blue in the presence of sodium borohydride ($NaBH_4$) and white light at room temperature. First, 3 mL of diluted methylene blue was analyzed in the visible ultraviolet, two optical absorption peaks appeared at 611 nm and 663 nm. To study the catalytic effect of biosynthesized silver nanoparticles Ag_2O NPs, 2.25 ml of $NaBH_4$ solution (6×10^{-6} M) (considered as a reducing agent) was added to 3 mL of methylene blue solution (2×10^{-6} M), then the addition of biosynthesized silver nanoparticles (80 mg/L). The degradation process was monitored by spectrophotometry in a wavelength range of 400-800 nm every 5 min for 30 min. The decolorization was observed by the decrease in the absorbance intensity of the solution at maximum length (λ_{max}). The experiments evaluated the catalytic efficiency of the biosynthesized Ag_2O NPs nanocatalysts.

3. Results and Discussion

3.1. Characterization of Silver Oxide Nanoparticles Ag_2O NPs

3.1.1 UV- vis spectroscopy and optical bandgap

Preliminary studies suggest that phytochemical screening of *H. hirsuta* plant extract evidences the presence of polyphenols, flavonoids and condensed tannins [28]. The as-prepared colloidal solution of Ag_2O and the plant extract were analyzed by UV-Vis spectroscopy (see Figure 1). In fact, the spectrum of plant extract showed two peaks at 300 nm and 670 nm. After the reaction, the spectrum of Ag_2O NPs revealed a peak located at 430 nm. This peak corresponds to the characteristic surface plasmon resonance absorption band of Ag_2O [29].

3.1.2 Determination of the optical bandgap

In general, the optical band gap of a semiconductor can be determined by plotting the absorption coefficient against the photon energy which could be estimated using Tauc's formula (Equation (1)) [30] :

$$(\alpha h\nu) = K\left(h\nu - E_g\right)^n \quad (1)$$

where α is the absorption coefficient, $h\nu$ is the incident photon energy, K is a constant, E_g is the optical band gap in electron volts (eV) and n is an exponent that can take two values depending on the nature of the electronic transition, *i.e.* n = 2 for a direct transition, and n = 1/2 for an indirect transition as shown in Figure 2 and Figure 3 [31,32].

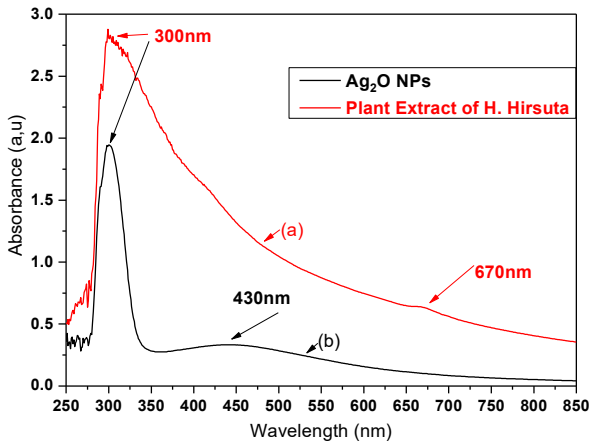

Figure 1. UV-visible Spectrum (b) of Ag_2O NPs biosynthesized and (a) of plant Extract of *H. hirsuta*.

3.1.3 Estimation of the Urbach energy

The Urbach energy refers to the width of the band tails of localized states. The Urbach energy is determined from Equation (2) from the slope of the linear part of the plot of ln against the photon energy (Figure 4) [33]. The results of the direct and indirect bandgap, as well as the Urbach energy, are presented in Table 1.

$$\ln(\alpha) = \frac{h\nu}{Eu} + \ln(\alpha_0) \quad (2)$$

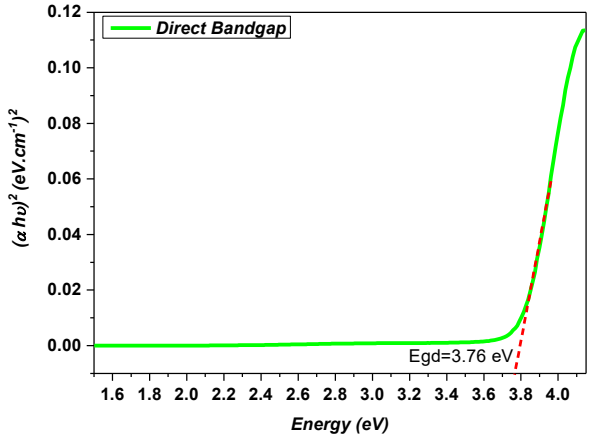

Figure 2. Determination of the optical bandgap for the direct transition using the Tauc method.

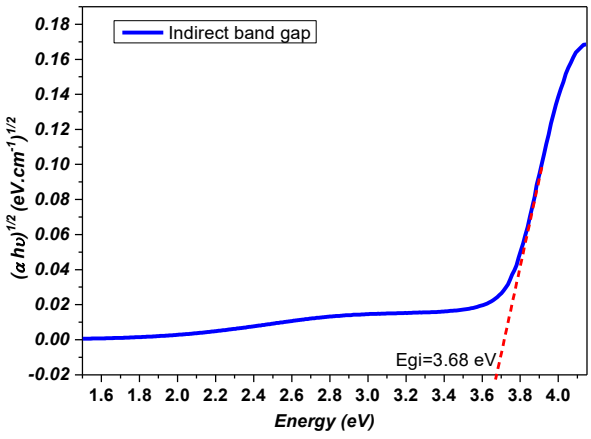

Figure 3. Determination of the optical bandgap for the indirect transition using the Tauc method.

3.1.4 Fourier transform infrared spectroscopy (FTIR)

Identification by FTIR analysis shows the potential presence of reducing and stabilizing biomolecules in the extract of the plant *H. hirsuta*. In the resulting FTIR spectrum (Figure 5) several absorption bands are presented, which correspond to the functional groups of the biomolecules existing in the plant extract of *H. hirsuta*. Seven main absorption peaks were observed, the broad peak centered at 3400 and 3533 cm^{-1} are assigned to the O–H stretching vibrations of flavonoids and alkaloids, the intense peak at 1123 and 1687 cm^{-1} are due to

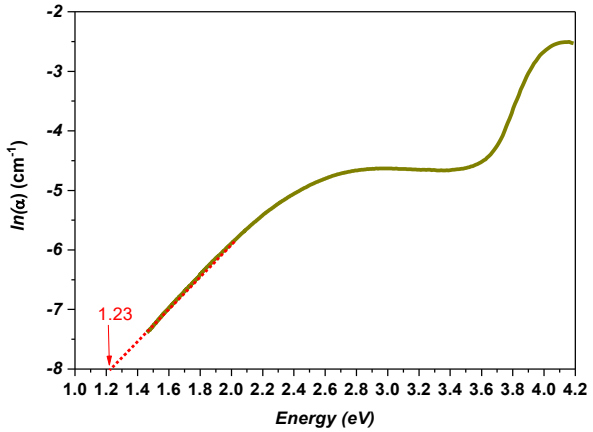

Figure 4. Plot ln(α) versus energy: Urbach energy estimate for biosynthesized Ag_2O NPs.

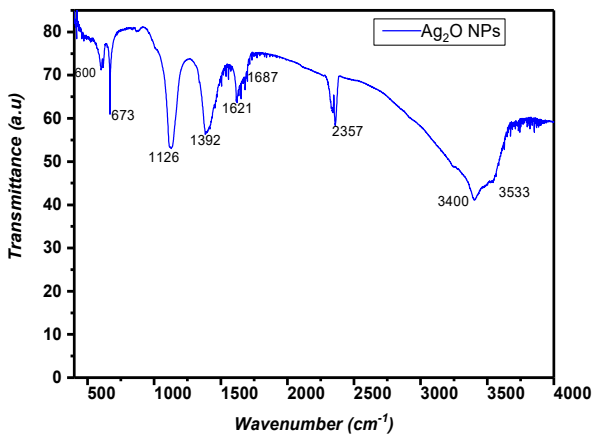

Figure 5. FTIR spectrum of nanoparticles biosynthesized Ag_2O NPs.

Table 1. The values of direct, indirect bandgap and Urbach energy of the biosynthesized Ag_2O NPs.

Energy (eV)		
Direct Optical bandgap	Indirect Optical bandgap	Urbach energy
3.76	3.68	1.23

the C=O stretching and N–H bending vibrations of the primary amide group which often exist in proteins [34]. The two peaks located at 1392 cm^{-1} pharmaceuticals and medicine and 1621 cm^{-1} are attributed to Nitro-banding NO and COC stretching vibrations of the aromatic ring respectively [35]. In addition, the peaks located at 673 cm^{-1} and 650 cm^{-1} were respectively attributed to Ag–O bending vibrations and C–H out-of-plane bending vibrations [25]. The FTIR results show that the extract of *H. hirsuta* plant contains many different functional groups, such as: carboxyls, carbonyls, amides and phenols, which could be used as bioreducing and capping agents for the synthesis of Ag_2O NPs [28].

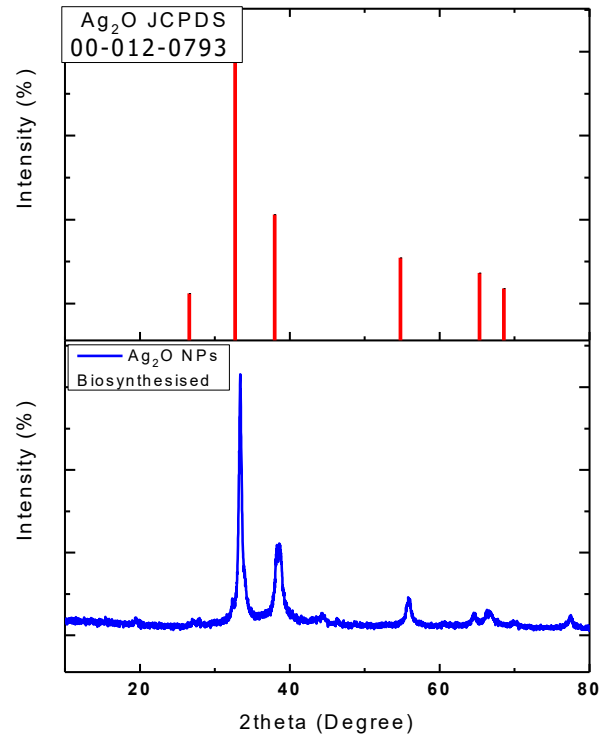

Figure 6. XRD diagram of biosynthesized Ag_2O NPs.

3.1.5 X-ray diffraction (XRD)

The X-ray diffraction pattern of biosynthesized Ag_2O NPs is shown in Figure 6. Several Bragg reflection peaks were observed in the XRD pattern located at 2 values of 27.28°, 33.36°, 55.93°, 66.52° and 70.01° corresponding to the (110), (111), (220), (311) and (222) planes of Ag_2O silver oxide of face-centered cubic crystal structure (JCPDS, File No. 00-012-0793) [20]. The crystallite size of the biosynthesized Ag_2O NPs nanoparticles was calculated using Scherrer's formula Equation (3), considering the most intense peak located at the θ value of 33.45°:

$$D = \frac{0.9 \times \lambda}{\beta \times \cos\theta} \quad (3)$$

where D is the crystal size (nm), β is the total width at half the diffraction peak maximum

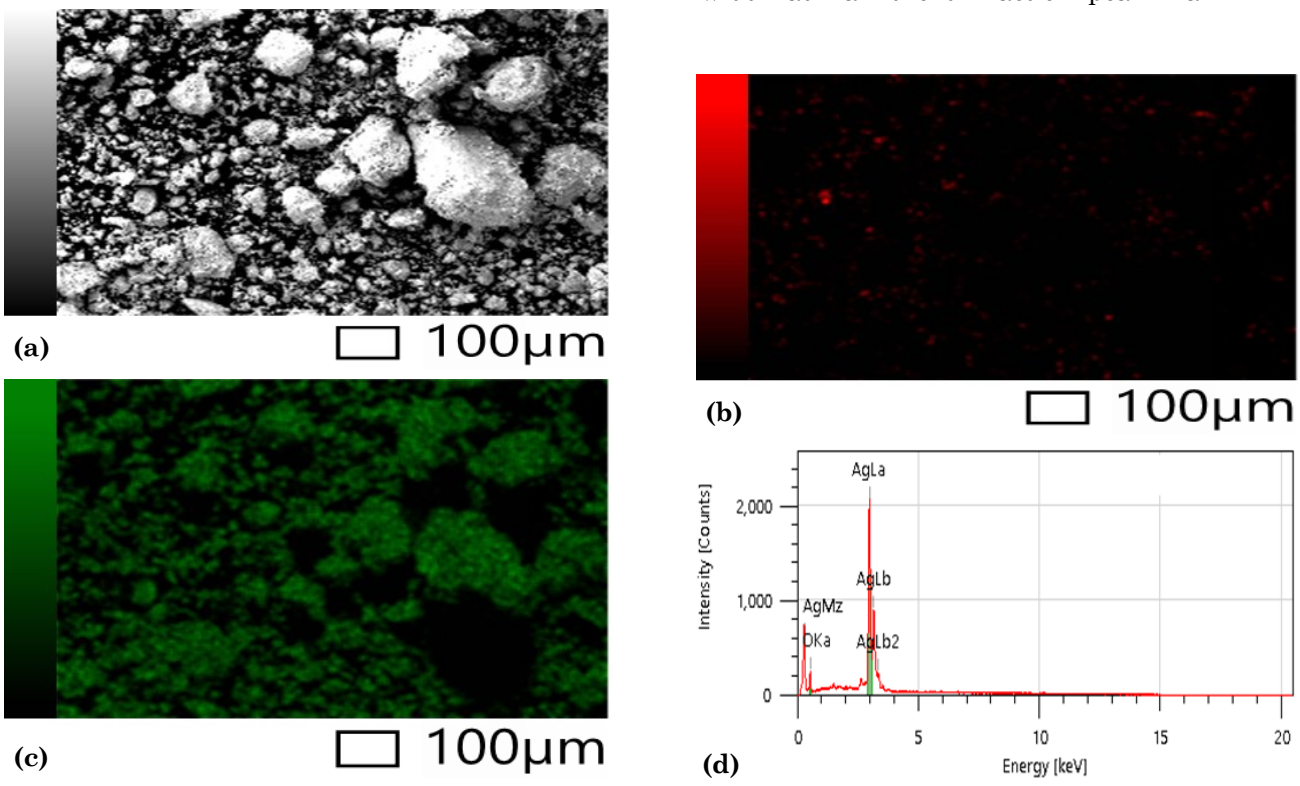

Figure 7. (a) FESEM images of spherical biosynthesized Ag_2O, (b,c) corresponding EDS elemental mapping of O and Ag, (d) EDS spectrum of NPs Ag_2O biosynthesized.

(FWHM) of the most intense diffraction peak, λ is the X-ray wavelength (for Cu-Kα λ=1.5406 Å), and θ is the Bragg diffraction angle. Its value was 17.16 nm, and the average crystal size is 15.51 nm.

3.1.6 Morphological study by scanning electron microscopy (SEM)

SEM was used to study the morphology of Ag_2O NPs and their morphological size. In Figure 7 (a-c) the SEM images and elemental mapping of Ag_2O NPs. It was observed that most of them have a spherical shape. And in Figure 7 (d), EDS analysis indicates that the elements present in the synthesized product are oxygen O and silver Ag, the element Ag more abandoning than the element O.

3.2 Catalytic Activity for BM Degradation

The catalytic hydrolysis of MB dye in the presence of $NaBH_4$ was examined to confirm the catalytic activity of Ag_2O NPs. The catalytic degradation is monitored by UV-Vis spectroscopy. By adding the Ag_2O nanoparticles into the reaction mixture, the catalytic reduction of the dye takes place after a few minutes. The strong blue color of the MB solution fades and becomes colorless after 35 minutes during the degradation process Figure 8. The degradation efficiency is calculated by the following formula (Equation (4)):

$$D\% = \frac{(C_0 - C_t)}{C_0} \times 100 \qquad (4)$$

where C_0 is the initial concentration of MB and C_t the immediate concentration in the sample.

The presence of amide groups of Ag_2O NPs in the electron transfer of BH_4^- anions to MB cations, which increases with time, which was also similar to the previously reported Ag_2O NPs [36,37]. The initial absorption peak at 663 nm was attenuated with time, which demonstrates the catalytic activity of the Ag_2O NPs product (Figure 10). Figure 9 schematically shows the mechanism of the catalytic degradation process of MB dye. The number of cycles of use of biosynthesized Ag_2O nanoparticles for the photocatalysis of MB is equal to 4 (Figure 11).

Analysis of the kinetic data of the degradation reaction showed that the reaction kinetics is pseudo-first order. The reaction rate is determined by the following relationship:

$$\ln\left(\frac{C_t}{C_0}\right) = \ln\left(\frac{A_t}{A_0}\right) = -K_{app} \times t \qquad (5)$$

where C_t (A_t) and C_0 (A_0) represent the concentration (absorbance) of the MB dye after and before degradation, respectively. The slope of

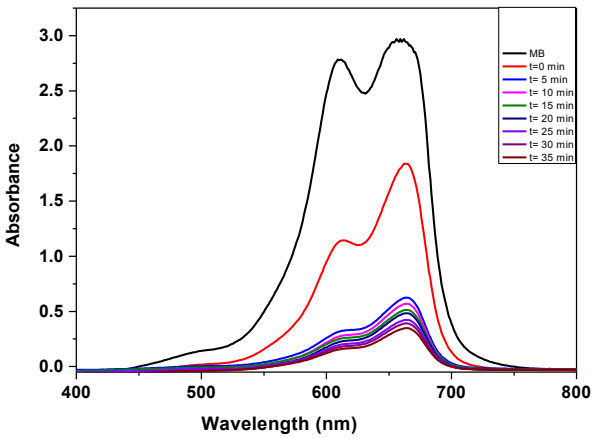

Figure 8. UV-vis spectrum for the reduction of MB using biosynthesized Ag_2O NPs.

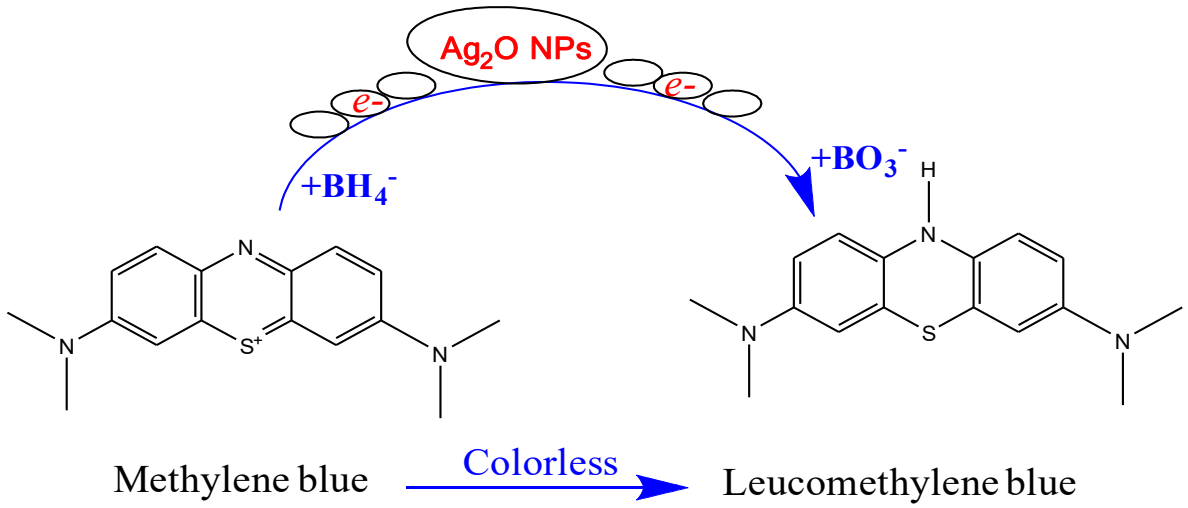

Figure 9. Schematic of the catalytic degradation process of MB dye by Ag_2O NPs.

the curve determines the value of K_{app} (min^{-1}). The linear plot of ln (C_t/C_0) versus time (Figure 12) affirms the kinetic theory, where the value of K_{app} is 0.020 min^{-1} [36,38]. The catalytic performance of silver oxide nanoparticles is related to their specific morphology that allows the rapid movement of electrons on the catalyst surface, and their small size (average size of 15.51 nm) ensures a large specific surface area that facilitates the dye degradation reaction by the silver oxide nanocatalyst, which reaches the rate of 88.6% after a duration of 35 min. Then, these two characteristics of biosynthesized Ag_2O NPs accelerate the degradation process of the methylene blue dye.

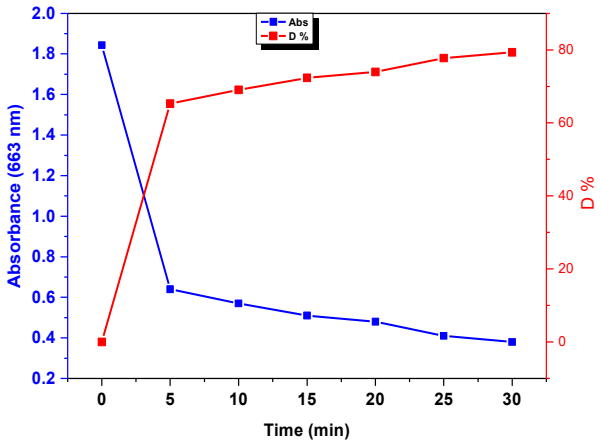

Figure 10. The evolution of absorbance (663 nm) and degradation (D%) of methylene blue dye versus time.

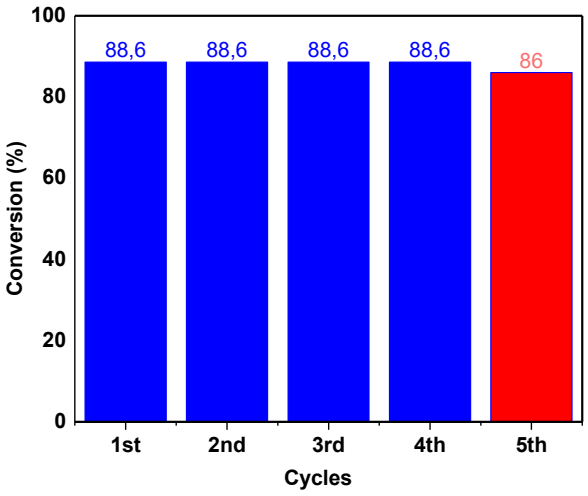

Figure 11. Percentage conversion of methylene blue in each catalytic cycle after 35 min.

4. Conclusion

In this study, for the first time the green synthesis of silver oxide nanoparticles was successfully achieved using the aqueous extract of the wild plant *Herniaria hirsuta*. The process is easy, fast, cheap, environmentally friendly, and does not require any organic solvent or surfactant. Therefore, this synthesis method is more advantageous than traditional methods for the synthesis of Ag_2O nanoparticles. The shape of the biosynthesized Ag_2O nanoparticles is almost spherical, of cubic crystalline nature, and the average crystal size is 15.51 nm, which implies that they will be of great interest to the research community. Moreover, the Ag_2O nanoparticles prepared exhibit a better catalytic activity for the degradation of the MB dye under standard conditions which approached the rate of 89% due to their morphology and their small size. The biosynthesized Ag_2O NPs are of great importance in wastewater treatment (dye degradation), medicine, cosmetics, paints, plastics and textiles.

Acknowledgment

The authors would like to thank the Centre for Research and Analysis and Characterisation (CRAC) at the Faculty of Science and Technology of Settat, which provided us with the necessary analyses.

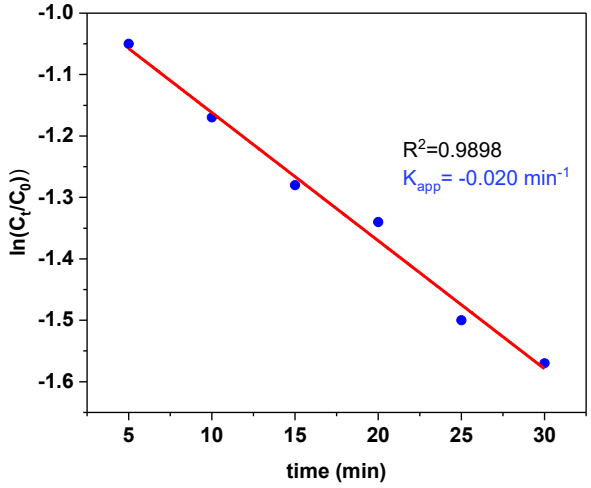

Figure 12. Plot of ln (C_t/C_0) versus time for the reaction of catalytic reduction of MB with Ag_2O NPs.

References

[1] Laouini, S.E., Bouafia, A., Soldatov, A.V., Algarni, H., Tedjani, M.L., Ali, G.A., Barhoum, A. (2021). Green Synthesized of Ag/Ag_2O Nanoparticles Using Aqueous Leaves Extracts of Phoenix dactylifera L. and Their Azo Dye Photodegradation. *Membranes*, 11(7), 468. DOI: 10.3390/membranes11070468.

[2] Chuto, G., Chaumet-Riffaud, P. (2010). Les nanoparticules. *Médecine Nucléaire*, 34(6), 370-376. DOI:10.1016/j.mednuc.2010.03.003.

[3] Lateef, A., Folarin, B.I., Oladejo, S.M., Akinola, P.O., Beukes, L.S., Gueguim-Kana, E.B. (2018). Characterization, antimicrobial, antioxidant, and anticoagulant activities of silver nanoparticles synthesized from Petiveria alliacea L. leaf extract. *Preparative Biochemistry and Biotechnology*, 48(7), 646-652. DOI:10.1080/10826068.2018.1479864.

[4] Boopathi, S., Gopinath, S., Boopathi, T., Balamurugan, V., Rajeshkumar, R., Sundararaman, M. (2012). Characterization and antimicrobial properties of silver and silver oxide nanoparticles synthesized by cell-free extract of a mangrove-associated Pseudomonas aeruginosa M6 using two different thermal treatments. *Industrial & Engineering Chemistry Research*, 51(17), 5976-5985. DOI: 10.1021/ie3001869

[5] Li, R., Chen, Z., Ren, N., Wang, Y., Wang, Y., Yu, F. (2019). Biosynthesis of silver oxide nanoparticles and their photocatalytic and antimicrobial activity evaluation for wound healing applications in nursing care. *Journal of Photochemistry and Photobiology B: Biology*, 199, 111593. DOI: 10.1016/j.jphotobiol.2019.111593

[6] Ovais, M., Khalil, A.T., Islam, N.U., Ahmad, I., Ayaz, M., Saravanan, M., Shinwari, Z.K., Mukherjee, S. (2018). Role of plant phytochemicals and microbial enzymes in biosynthesis of metallic nanoparticles. *Applied Microbiology and Biotechnology*, 102(16), 6799-6814. DOI: 10.1007/s00253-018-9146-7

[7] Shanthi, S., Jayaseelan, B.D., Velusamy, P., Vijayakumar, S., Chih, C.T., Vaseeharan, B. (2016). Biosynthesis of silver nanoparticles using a probiotic Bacillus licheniformis Dahb1 and their antibiofilm activity and toxicity effects in Ceriodaphnia cornuta. *Microbial Pathogenesis*, 93, 70-77. DOI: 10.1016/j.micpath.2016.01.014.

[8] Ida, Y., Watase, S., Shinagawa, T., Watanabe, M., Chigane, M., Inaba, M., Tasaka, A., Izaki, M. (2008). Direct electrodeposition of 1.46 eV bandgap silver (I) oxide semiconductor films by electrogenerated acid. *Chemistry of Materials*, 20(4), 1254-1256. DOI: 10.1021/cm702865r.

[9] Xaba, T., Moloto, M.J., Al-Shakban, M., Malik, M.A., O'Brien, P., Moloto, N. (2017). The effect of temperature on the growth of Ag2O nanoparticles and thin films from bis (2-hydroxy-1-naphthaldehydato) silver (I) complex by the thermal decomposition of spin–coated films. *Materials Science in Semiconductor Processing*, 71, 109-115. DOI: 10.1016/j.mssp.2017.07.015.

[10] Torabi, S., Mansoorkhani, M.J.K., Majedi, A., Motevalli, S. (2020). Synthesis, medical and photocatalyst applications of nano-Ag2O. *Journal of Coordination Chemistry*, 73(13), 1861-1880. DOI: 10.1080/00958972.2020.1806252..

[11] Pan, J., Sun, Y., Wang, Z., Wan, P., Liu, X., Fan, M. (2007). Nano silver oxide (AgO) as a super high charge/discharge rate cathode material for rechargeable alkaline batteries. *Journal of Materials Chemistry*, 17(45), 4820-4825. DOI: 10.1039/B711373K.

[12] Tominaga, J. (2003). The application of silver oxide thin films to plasmon photonic devices. *Journal of Physics: Condensed Matter*, 15(25), R1101. DOI: 10.1088/0953-8984/15/25/201.

[13] Wren, S., Minelli, C., Pei, Y., Akhtar, N. (2020). Evaluation of particle size techniques to support the development of manufacturing scale nanoparticles for application in pharmaceuticals. *Journal of Pharmaceutical Sciences*, 109(7), 2284-2293. DOI: 10.1016/j.xphs.2020.04.001.

[14] Russell, A.D., Hugo, W.B. (1994). 7 antimicrobial activity and action of silver. *Progress in Medicinal Chemistry*, 31, 351-370. DOI: 10.1016/s0079-6468(08)70024-9.

[15] Esmaile, F., Koohestani, H., Abdollah-Pour, H. (2020). Characterization and antibacterial activity of silver nanoparticles green synthesized using Ziziphora clinopodioides extract. *Environmental Nanotechnology, Monitoring & Management*, 14, 100303. DOI: 10.1016/j.enmm.2020.100303

[16] Lateef, A., Folarin, B.I., Oladejo, S.M., Akinola, P.O., Beukes, L.S., Gueguim-Kana, E.B. (2018). Characterization, antimicrobial, antioxidant, and anticoagulant activities of silver nanoparticles synthesized from Petiveria alliacea L. leaf extract. *Preparative Biochemistry and Biotechnology*, 48(7), 646-652. DOI: 10.1080/10826068.2018.1479864

[17] Shah, A., Haq, S., Rehman, W., Waseem, M., Shoukat, S., Rehman, M.U. (2019). Photocatalytic and antibacterial activities of paeonia emodi mediated silver oxide nanoparticles. *Materials Research Express*, 6(4), 045045. DOI: 10.1088/2053-1591/aafd42

[18] Rashmi, B.N., Harlapur, S.F., Avinash, B., Ravikumar, C.R., Nagaswarupa, H.P., Kumar, M.R.A., Gurushantha, K., Santosh, M.S. (2020). Facile green synthesis of silver oxide nanoparticles and their electrochemical, photocatalytic and biological studies. *Inorganic Chemistry Communications*, 111, 107580. DOI: 10.1016/j.inoche.2019.107580.

[19] Ravichandran, S., Paluri, V., Kumar, G., Loganathan, K., Kokati Venkata, B.R. (2016). A novel approach for the biosynthesis of silver oxide nanoparticles using aqueous leaf extract of Callistemon lanceolatus (Myrtaceae) and their therapeutic potential. *Journal of Experimental Nanoscience*, 11(6), 445-458. DOI: 10.1080/17458080.2015.1077534.

[20] Manikandan, V., Velmurugan, P., Park, J.H., Chang, W.S., Park, Y.J., Jayanthi, P., Cho, M., Oh, B.T. (2017). Green synthesis of silver oxide nanoparticles and its antibacterial activity against dental pathogens. *3 Biotech*, 7(1), 72. DOI: 10.1007/s13205-017-0670-4

[21] Menon, S., Rajeshkumar, S., Kumar, V. (2017). A review on biogenic synthesis of gold nanoparticles, characterization, and its applications. *Resource-Efficient Technologies*, 3(4), 516-527. DOI: 10.1016/j.reffit.2017.08.002.

[22] Samuel, M.S., Jose, S., Selvarajan, E., Mathimani, T., Pugazhendhi, A. (2020). Biosynthesized silver nanoparticles using Bacillus amyloliquefaciens; Application for cytotoxicity effect on A549 cell line and photocatalytic degradation of p-nitrophenol. *Journal of Photochemistry and Photobiology B: Biology*, 202, 111642. DOI: 10.1016/j.jphotobiol.2019.111642.

[23] Rajendran, K., Karunagaran, V., Mahanty, B., Sen, S. (2015). Biosynthesis of hematite nanoparticles and its cytotoxic effect on HepG2 cancer cells. *International Journal of Biological Macromolecules*, 74, 376-381. DOI: 10.1016/j.ijbiomac.2014.12.028.

[24] Wang, L., Hu, C., Shao, L. (2017). The antimicrobial activity of nanoparticles: present situation and prospects for the future. *International journal of nanomedicine*, 12, 1227. DOI: 10.2147/IJN.S121956.

[25] Fairuzi, A.A., Bonnia, N.N., Akhir, R.M., Abrani, M.A., Akil, H.M. (2018). Degradation of methylene blue using silver nanoparticles synthesized from imperata cylindrica aqueous extract. *IOP Conference Series: Earth and Environmental Science,* 105(1), 012018. DOI: 10.1088/1755-1315/105/1/012018.

[26] Adeyi, A.A., Jamil, S.N.A.M., Abdullah, L.C., Choong, T.S.Y., Lau, K.L., Abdullah, M. (2019). Adsorptive removal of methylene blue from aquatic environments using thiourea-modified poly (acrylonitrile-co-acrylic acid). *Materials*, 12(11), 1734. DOI: 10.3390/ma12111734

[27] Mantasha, I., Saleh, H.A., Qasem, K.M., Shahid, M., Mehtab, M., Ahmad, M. (2020). Efficient and selective adsorption and separation of methylene blue (MB) from mixture of dyes in aqueous environment employing a Cu (II) based metal organic framework. *Inorganica Chimica Acta*, 511, 119787. DOI: 10.1016/j.ica.2020.119787

[28] Ammor, K., Bousta, D., Jennan, S., Bennani, B., Chaqroune, A., Mahjoubi, F. (2018). Phytochemical Screening, Polyphenols Content, Antioxidant Power, and Antibacterial Activity of Herniaria hirsuta from Morocco. *The Scientific World Journal*, 2018, 7470384. DOI: 10.1155/2018/7470384.

[29] Dhoondia, Z.H., Chakraborty, H. (2012). Lactobacillus mediated synthesis of silver oxide nanoparticles. *Nanomaterials and Nanotechnology*, 2, 15. DOI: 10.5772/55741.

[30] De, A.K., Majumdar, S., Pal, S., Kumar, S., Sinha, I. (2020). Zn doping induced band gap widening of Ag2O nanoparticles. *Journal of Alloys and Compounds*, 832, 154127. DOI: 10.1016/j.jallcom.2020.154127.

[31] Liu, Y., Li, P., Xue, R., Fan, X. (2020). Research on catalytic performance and mechanism of Ag2O/ZnO heterostructure under UV and visible light. *Chemical Physics Letters*, 746, 137301. DOI: 10.1016/j.cplett.2020.137301.

[32] Mohamed, R.M., Ismail, A.A., Kadi, M.W., Alresheedi, A.S., Mkhalid, I.A. (2020). Facile Synthesis of Mesoporous Ag2O–ZnO Heterojunctions for Efficient Promotion of Visible Light Photodegradation of Tetracycline. *ACS Omega*, 5(51), 33269-33279. DOI: 10.1021/acsomega.0c04969.

[33] Kandi, D., Mansingh, S., Behera, A., Parida, K. (2021). Calculation of relative fluorescence quantum yield and Urbach energy of colloidal CdS QDs in various easily accessible solvents. *Journal of Luminescence*, 231, 117792. DOI: 10.1016/j.jlumin.2020.117792.

[34] Dharmaraj, D., Krishnamoorthy, M., Rajendran, K., Karuppiah, K., Annamalai, J., Durairaj, K.R., Santhiyagu, P., Ethiraj, K. (2021). Antibacterial and cytotoxicity activities of biosynthesized silver oxide (Ag2O) nanoparticles using Bacillus paramycoides. *Journal of Drug Delivery Science and Technology*, 61, 102111. DOI: 10.1016/j.jddst.2020.102111.

[35] Mourdikoudis, S., Pallares, R.M., Thanh, N.T. (2018). Characterization techniques for nanoparticles: comparison and complementarity upon studying nanoparticle properties. *Nanoscale*, 10(27), 12871-12934. DOI: 10.1039/C8NR02278J.

[36] Fairuzi, A.A., Bonnia, N.N., Akhir, R.M., Abrani, M.A., Akil, H.M. (2018). Degradation of methylene blue using silver nanoparticles synthesized from imperata cylindrica aqueous extract. *IOP Conference Series: Earth and Environmental Science,* 105(1), 012018. DOI: 10.1088/1755-1315/105/1/012018.

[37] Nasrollahzadeh, M., Issaabadi, Z., Sajadi, S.M. (2019). Green synthesis of Cu/Al2O3 nanoparticles as efficient and recyclable catalyst for reduction of 2, 4-dinitrophenylhydrazine, Methylene blue and Congo red. *Composites Part B: Engineering*, 166, 112-119. DOI: 10.1016/j.compositesb.2018.11.113.

[38] Raj, S., Singh, H., Trivedi, R., Soni, V. (2020). Biogenic synthesis of AgNPs employing Terminalia arjuna leaf extract and its efficacy towards catalytic degradation of organic dyes. *Scientific Reports*, 10(1), 1-10. DOI: 10.1038/s41598-020-66851-8.

[39] Vanaja, M., Paulkumar, K., Baburaja, M., Rajeshkumar, S., Gnanajobitha, G., Malarkodi, C., Sivakavinesan, M., Annadurai, G. (2014). Degradation of methylene blue using biologically synthesized silver nanoparticles. *Bioinorganic Chemistry and Applications*, 2014, 742346. DOI: 10.1155/2014/742346.